Molecular-Level Mechanical Instabilities and Enhanced Self-Diffusion in Flowing Liquids

Dennis L. Malandro and Daniel J. Lacks

Department of Chemical Engineering, Tulane University, New Orleans, Louisiana 70118

(Received 27 July 1998)

Molecular simulations show that shear strains arising from liquid flow cause local minima of the potential-energy surface to disappear, leading to mechanical instabilities which force the system towards alternate local minima. Associated with these mechanical instabilities are irreversible atomic displacements, which are strain activated rather than thermally activated. These displacements generate self-diffusion in excess of that from thermal-activation alone and give rise to the shear-enhanced self-diffusion known to occur in flowing liquids and concentrated suspensions of particles. The magnitude of this enhancement is shown to decrease with increasing temperature and strain rate. [S0031-9007(98)07979-4]

PACS numbers: 61.20.Ja, 66.10.Cb

The presence of shear flow is known to affect the diffusion constants of a system. On a molecular level, nonequilibrium molecular dynamics (NEMD) simulations have shown that diffusion constants in liquids can increase significantly within shear flows [1–5]. Similar effects have been observed in systems of particles suspended in liquids, both in experiments [6–10] and simulations [11–13].

The present investigation addresses the effects of shear flow on self-diffusion in liquids using the inherent structure formalism [14], which separates the dynamics of liquids into vibrational motion within one local potential energy minimum (an "inherent structure"), and diffusive motion between different local minima. The rate of diffusion is in this way related to the frequency of transitions between local minima. The simulations are carried out for a system composed of 256 atoms of mass m, which interact with a Lennard-Jones potential characterized by the parameters ε and σ and truncated at the distance 2.5σ; the characteristic time for the system $\tau = (m\sigma^2/\varepsilon)^{1/2}$. The simulations are carried out for a density $\rho = 0.8442\sigma^{-3}$, which is the triple point density of the Lennard-Jones system (note that the qualitatively different effects of shear seen in gas phase systems [3,15] are not addressed here).

To understand the physical origins of the shear-enhanced self-diffusion, the behavior of the system under shear is examined first in the case that it always remains at a potential energy minimum (i.e., there is no thermal energy). An initial local potential energy minimum for a cubic simulation cell is generated by quenching a liquid to zero temperature, after which the shear strain, ε_{xy}, of the simulation cell is increased in increments of 0.1% (the shear is along the x direction). After each strain increment, the potential energy is reminimized with respect to the atomic coordinates (at constant strain). The average atomic displacements with respect to the initial cubic cell atomic positions are obtained at each strain (the relevant coordinates are those with respect to the center of mass).

The resulting atomic displacements (with the system always at a potential energy minimum) consist of regions in which there is little change in the displacements with strain, punctuated by discontinuous jumps in the displacements, as shown in Fig. 1(a). To determine the cause of the discontinuous jumps, which account for almost all of the atomic displacements, properties of the potential energy landscape were probed. As shown in Fig. 2, the discontinuous jumps in atomic displacements coincide with the decrease to zero of the following properties: the height of a barrier (i.e., saddle point), the curvature of the potential energy surface (along one direction) at the positions of both the minimum and the barrier, and the distance between the minimum and the barrier. These trends are indicative of the disappearance of a local energy minimum which renders the system mechanically unstable, as shown schematically in Fig. 3. The discontinuous jumps in atomic positions thus arise from mechanical instabilities and subsequent relaxation to different energy minima and are strain activated rather than thermally activated. The instabilities are irreversible, as the new potential energy minimum will in general remain stable as the strains are reversed [see Figs. 2(a) and 2(c)]. The instabilities are also found to be localized to a small number of atoms. These shear-induced mechanical instabilities are analogous to the pressure-induced mechanical instabilities in glasses examined previously [16,17].

The atomic displacements associated with the mechanical instabilities correspond to steps in a random walk (in the directions perpendicular to the shear); the sum of these steps gives rise to self-diffusion which is strain activated rather than thermally activated. Although these results are time independent, Einstein relations can be used to extract the quantities $D_{yy}(T = 0)/\gamma$ and $D_{zz}(T = 0)/\gamma$,

$$\langle \Delta y^2 \rangle = 2D_{yy}t = 2\left(\frac{D_{yy}}{\gamma}\right)\varepsilon_{xy}\,,$$
$$\langle \Delta z^2 \rangle = 2D_{zz}t = 2\left(\frac{D_{zz}}{\gamma}\right)\varepsilon_{xy}\,, \tag{1}$$

 0031-9007/98/81(25)/5576(4)$15.00

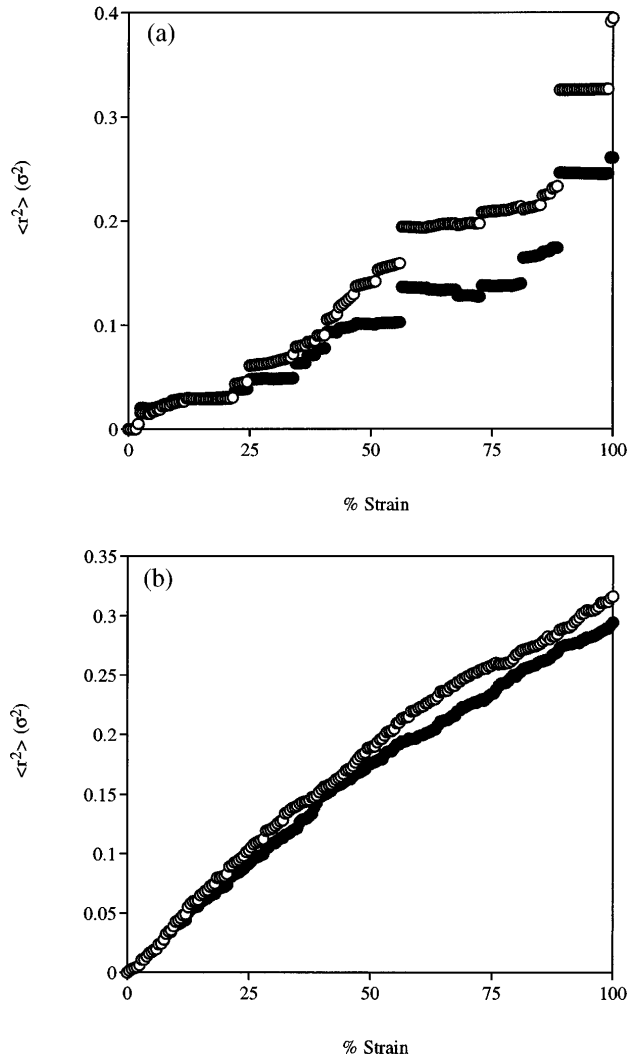

FIG. 1. Mean-square displacement of atomic positions corresponding to the potential energy minimum, as a function of shear strain. Filled circles: $\langle y^2 \rangle$; open circles: $\langle z^2 \rangle$. (a) A single simulation; (b) average of 29 simulations.

where the strain rate $\gamma = \varepsilon_{xy}/t$ and D_{ii} is the diffusion constant in the i direction (note that the lack of thermal effects here corresponds to the temperature $T = 0$). From an average of the results of 29 systems [Fig. 1(b)], it is found that $D_{yy}(0) \approx 0.16\gamma\sigma^2$ and $D_{zz}(0) \approx 0.15\gamma\sigma^2$.

These strain-activated contributions to diffusion will augment the usual thermally activated contributions, but the two contributions do not operate independently. This effect can be understood as follows: A local minimum remains stable on average for some strain interval $\Delta\varepsilon_{xy}$ or time interval $\Delta t = \Delta\varepsilon_{xy}/\gamma$. If the system does not undergo a thermally activated transition within Δt, it will (on average) undergo a strain-activated transition. However, if the system does undergo a thermally activated transition during Δt, the strain-activated transition from that local minimum is precluded. Thermally activated transitions thus act to decrease the frequency of strain-activated transitions, which reduces the strain-activated contribution to diffusion; i.e., $\partial D_{ii}/\partial\gamma$ will decrease with increasing temperature and equal $D_{ii}(0)/\gamma$ only as $T \to 0$.

Both the strain-activated and thermally activated contributions to diffusion will decrease with high strain rates. The frequency of strain-activated transitions decreases with high strain rates for the following reason: After a local minimum disappears due to shear, the system may not have time to relax to the new minimum before the new minimum also disappears due to shear. The frequency of thermally activated transitions decreases with high strain rates because the system may not have time to traverse a low energy barrier before the shear-induced changes in the potential energy surface cause the barrier to become large. The shear enhancement of diffusion, $\partial D_{ii}/\partial\gamma$, is thus greatest for $\gamma \to 0$ and $T \to 0$.

To demonstrate the validity of the proposed mechanism for enhanced self-diffusion in liquids, NEMD simulations are carried out to determine the self-diffusion constants as a function of shear rate and temperature, using the sllod equations of motion with the temperature maintained by a Gaussian thermostat [18] (previous NEMD simulations [1–5] did not address this temperature dependence). At lower temperatures ($T \leq 0.3\varepsilon/k$), the system is intermittently heated and recooled in order to avoid crystallization. The diffusion constants D_{yy} and D_{zz} are determined from Einstein relations. The simulations are carried out for 10 to 15 values of γ at each temperature, for values $0 < \gamma < \gamma_{\max}$, where $\gamma_{\max}$ ranges from $0.03\tau^{-1}$ at the lower temperatures to $0.3\tau^{-1}$ at higher temperatures. The results for D_{ii} are fit to a polynomial in γ (first order for $T > 0.3\varepsilon/k$ and second order for $T \leq 0.3\varepsilon/k$), from which the slopes $\partial D_{ii}/\partial\gamma|_{\gamma\to 0}$ are obtained.

The NEMD results for $\partial D_{ii}/\partial\gamma|_{\gamma\to 0}$, given in Fig. 4, show that these values decrease with increasing temperature and, as $T \to 0$, extrapolate towards the values of $D_{ii}(0)/\gamma$ which are due to mechanical instabilities (as shown above). Also, previous NEMD simulations have shown that $\partial D_{ii}/\partial\gamma$ decreases with increasing γ [2,3,5]. These results thus corroborate the proposed mechanism for shear-enhanced self-diffusion in terms of mechanical instabilities.

We emphasize that the enhanced self-diffusion effect arises independently from the NEMD methodology. For example, our time-independent simulations, in which the system always remains at the potential energy minimum, exhibit strain-activated diffusion of the form $D \sim \sigma^2\gamma$ (see Fig. 1). These time-independent simulations correspond physically to NEMD simulations in the limits $T \to 0$ and $\gamma \to 0$ (i.e., it is in these limits that the system will remain at the potential energy minimum at all times).

The present results also have implications for very concentrated suspensions of particles undergoing shear flow. The particle packing in very concentrated suspensions will undergo mechanical instabilities with shear analogously to the atomic systems described above, giving rise to shear-enhanced self-diffusion in these systems (i.e., the

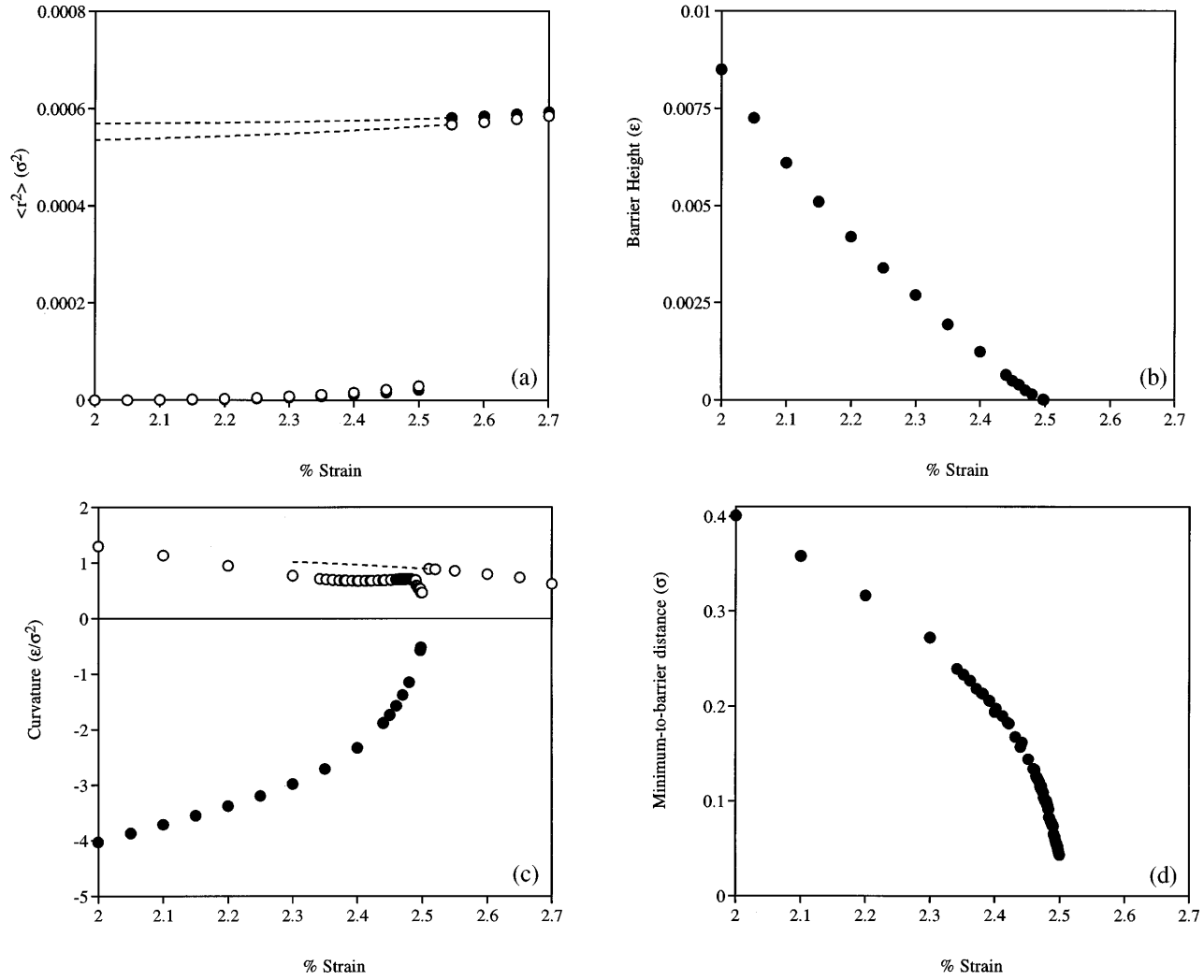

FIG. 2. Changes in characteristics of the potential-energy surface with shear strain. (a) Mean-square displacement of atomic positions along y (filled circles) and z (open circles); (b) a barrier height; (c) curvature along the reaction coordinate at the energy minimum (open circles) and at the barrier (filled circles); (d) distance between the energy minimum and the barrier. The dashed lines in (a) and (c) represent results obtained when the stresses are reversed.

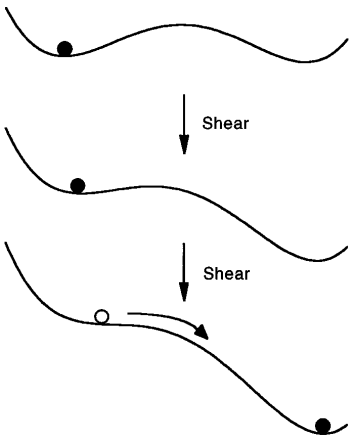

FIG. 3. Schematic representation of shear-induced mechanical instabilities in the potential-energy surface underlying liquids. The curves represent the potential energy along the relevant coordinate; the circles represent the state of the system.

"atoms" now represent "particles"). Previous theories of shear-enhanced diffusion in suspensions have focused on dilute suspensions and are thus based on discrete interparticle encounters [6,19–22]; the present mechanism in terms of mechanical instabilities is more appropriate for very concentrated systems, where the particles are essentially in constant contact rather than undergoing discrete encounters. The form of the diffusion constant $D \sim \sigma^2\gamma$ which arises from the mechanical instabilities in the same as that found experimentally in systems where thermally activated diffusion (i.e., Brownian motion) is negligible [7]. Brownian motion will decrease the value of $\partial D_{ii}/\partial\gamma$ in suspensions, for the same reason that thermally activated diffusion decreases the value of $\partial D_{ii}/\partial\gamma$ of liquids; however, the NEMD simulations are not relevant to suspensions due to the neglect of hydrodynamic effects.

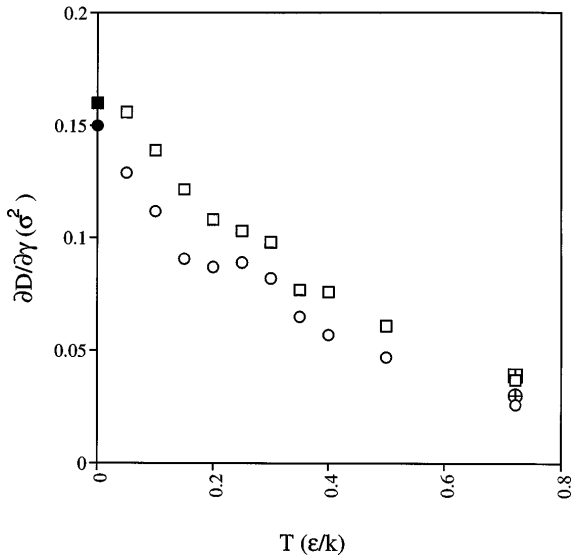

FIG. 4. Results for $\partial D_{yy}/\partial\gamma|_{\gamma\to 0}$ and $\partial D_{zz}/\partial\gamma|_{\gamma\to 0}$. The open symbols are the present NEMD results: The symbols with crosses are the results from Ref. [5], and the filled symbols are $D_{yy}(T=0)/\gamma$ and $D_{zz}(T=0)/\gamma$ obtained in the absence of thermal effects [see Fig. 1(b)]. Squares: $\partial D_{yy}/\partial\gamma|_{\gamma\to 0}$; circles: $\partial D_{zz}/\partial\gamma|_{\gamma\to 0}$.

Funding for this project was provided by the National Science Foundation (Grant No. DMR-9624808) and the Donors of the Petroleum Research Fund as administered by the American Chemical Society.

[1] D. M. Heyes, J. J. Kim, C. J. Montrose, and T. A. Litovitz, J. Chem. Phys. **73**, 3987 (1980).
[2] P. T. Cummings, B. Y. Wang, D. J. Evans, and K. J. Fraser, J. Chem. Phys. **94**, 2149 (1991).
[3] S. Sarman, D. J. Evans, and A. Baranyai, Phys. Rev. A **46**, 893 (1992).
[4] A. Baranyai and P. T. Cummings, Mol. Phys. **86**, 1314 (1995).
[5] W. C. Sandberg and D. M. Heyes, Mol. Phys. **85**, 635 (1995).
[6] E. C. Eckstein, D. G. Bailey, and A. H. Shapiro, J. Fluid Mech. **79**, 191 (1977).
[7] D. Leighton and A. Acrivos, J. Fluid Mech. **177**, 109 (1987); **181**, 415 (1987).
[8] X. Qiu, H. D. Ou-Yang, D. J. Pine, and P. M. Chaikin, Phys. Rev. Lett. **61**, 2554 (1988).
[9] J. R. Abbot, N. Tetlow, A. L. Graham, S. A. Altobelli, E. Fukushima, L. A. Mondy, and T. S. Stephens, J. Rheol. **35**, 773 (1991).
[10] C. Koh, P. Hookham, and L. G. Leal, J. Fluid Mech. **266**, 1 (1994).
[11] W. Xue and G. S. Grest, Phys. Rev. A **40**, 1709 (1989).
[12] T. N. Phung, J. F. Brady, and G. Bossis, J. Fluid Mech. **313**, 181 (1996); P. R. Nott and J. F. Brady, J. Fluid Mech. **275**, 157 (1994); G. Bossis and J. F. Brady, J. Chem. Phys. **87**, 5437 (1987).
[13] C. Chang and R. L. Powell, J. Fluid Mech. **281**, 51 (1994).
[14] F. H. Stillinger and T. A. Weber, Science **225**, 983 (1984); F. H. Stillinger, Science **267**, 1935 (1995).
[15] C. Marin and V. Garzo, Phys. Rev. E **57**, 507 (1998); V. Garzo and M. Lopez de Haro, Phys. Fluids A **4**, 1057 (1992).
[16] D. L. Malandro and D. J. Lacks, J. Chem. Phys. **107**, 5804 (1997).
[17] D. J. Lacks, Phys. Rev. Lett. **80**, 5385 (1998).
[18] D. J. Evans and G. P. Morriss, *Statistical Mechanics of Nonequilibrium Liquids* (Academic Press, London, 1990).
[19] J. F. Morris and J. F. Brady, J. Fluid Mech. **312**, 223 (1996).
[20] F. R. de Cunha and E. J. Hinch, J. Fluid Mech. **309**, 211 (1996).
[21] Y. Wang, R. Mauri, and A. Acrivos, J. Fluid Mech. **327**, 255 (1996).
[22] R. J. Phillips, R. C. Armstrong, R. A. Brown, A. L. Graham, and J. R. Abbot, Phys. Fluids A **4**, 30 (1992).